ELSEVIER

Journal of Chromatography A, 960 (2002) 97–108

JOURNAL OF CHROMATOGRAPHY A

www.elsevier.com/locate/chroma

Enantioseparation of various amino acid derivatives on a quinine based chiral anion-exchange selector at variable temperature conditions. Influence of structural parameters of the analytes on the apparent retention and enantioseparation characteristics ☆

W.R. Oberleitner, N.M. Maier*, W. Lindner[1,*]

Institute of Analytical Chemistry, University of Vienna, Währingerstrasse 38, A-1090 Vienna, Austria

Abstract

The influence of temperature on the performance of an enantioselective anion-exchange type chiral selector (SO) was systematically investigated. The resolution of the enantiomers of 23 *N*-acylated amino acids (selectands, SAs) on a covalently immobilized quinine *tert*.-butylcarbamate chiral stationary phase (CSP) was studied under linear chromatographic conditions over a temperature range of 0–85 °C with hydro–organic buffers (pH_a 6.0) as mobile phases. The apparent enantioseparation factors increased considerably at low column temperatures, indicating that enthalpic contributions are the dominating thermodynamic driving force for chiral recognition for all investigated SAs. Retention factors gave non-linear van't Hoff plots, while the corresponding apparent enantioseparation factors showed linear van't Hoff behavior. Correlations between magnitude and sign of the relative thermodynamic parameters of enantioselective adsorption ($\Delta\Delta G$, $\Delta\Delta H$ and $\Delta\Delta S$) and specific structural features of the analytes, i.e., steric and electronic nature of the various side chains and the *N*-acyl groups, are discussed with the aim to rationalize their possible contributions to the overall chiral recognition.

Keywords: Enantiomer separation; Chiral stationary phases, LC; Temperature effects; Apparent enantioselectivity; Apparent thermodynamics; Van't Hoff plots; Cinchona alkaloids; Amino acids

1. Introduction

Temperature has a major impact on retention, selectivity (enantioselectivity), resolution, and column efficiency for chromatographic enantiomer separation. Consequently, the variation of the column operation temperature has been frequently exploited as an optimization parameter in gas and liquid chromatographic separations of enantiomers [1–7]. As a special discipline, low-temperature liquid chromatography on chiral stationary phases (CSPs) has enabled the resolution of enantiomers which are configurationally labile at ambient temperatures [8]. Van't Hoff analysis of retention factors and enantioselectivity values derived from variable-temperature studies are routinely used to access thermodynamic functions of enantioselective adsorption, which may be interpreted in terms of mechanistic aspects of chiral recognition [6,9,10]. Numerous studies de-

☆ Dedicated to the memory of Josef Franz Karl Huber.

* Corresponding authors. Tel.: +43-1-4277-52373; fax: +43-1-4277-9523.

E-mail addresses: nmaier@anc.univie.ac.at (W. Lindner), wolfgang.lindner@univie.ac.at (W. Lindner).

[1] Tel.: +43-1-4277-52300; fax: +43-1-4277-3151826.

0021-9673/02/$ – see front matter
PII: S0021-9673(02)00244-3

voted to the elucidation of effects of temperature on the separation characteristics of chiral selector (SO) systems, such as proteins [9–12], crown ethers [13,14], cyclodextrins and cellulose derivatives [15–18], and π-donor–acceptor brush-type CSPs [16–23] have appeared. Nevertheless, relatively few contributions focused on the investigation of temperature effects of low-molecular-mass enantioselective ion-exchange SOs [12,24].

Jönsson et al. [11] and Fornstedt et al. [10] observed an unusual increase in enantioselectivity at increasing temperature for the separation of propranolol on a cellobiohydrolase (CBH I) type CSP using an acetate-buffered aqueous mobile phase. Non-linear plots of ln k vs. $1/T$ and linear ln α vs. $1/T$ plots were obtained. Karlsson and Aspegren [25] investigated the enantioselectivity of mosapride as a function of mobile phase pH and column temperature on an α_1-acid glycoprotein (AGP) phase and observed a reversal of elution order on varying both the pH and temperature. Naemura et al. [13] observed inversion of elution order for 2-aminopropan-1-ol in complexation with phenolic crown ethers at a temperature of ca. 6 °C. The effect of temperature in supercritical fluid chromatography (SFC) and high-performance liquid chromatography (HPLC) on the resolution and enantioselectivity of potassium channel activators was investigated by Smith et al. on a cellulose-carbamate type CSP [16]. Minor variations of functional groups within the analyte strongly influenced the thermodynamics of enantiomer separation. With π-donor–acceptor brush-type CSPs, Pirkle and Murray observed temperature- and solvent-dependent inversions of elution order [21], which was ascribed to selective desolvation phenomena of polar sites on the CSP. Papadopoulou-Mourkidou [19] described the effect of temperature on the enantioseparation of fenvalerate on a (*R*)-*N*-(3,5-dinitrobenzoyl)-phenylglycine derived CSP in a range between 2 and 35 °C. Enantioselectivity for enantiomers decreased as the column temperature was increased, while resolution was the best at 15 °C. Karlsson and Charron [12] used low-temperature chiral ion-pair chromatography with graphite-type stationary phases for the separation of amino alcohols and emphasized that gains in enantioselectivity at low temperatures are associated with a significant decrease in column-efficiencies. Linear van't Hoff plots were observed between −5 and 25 °C.

Under linear chromatographic conditions the temperature dependence of the retention of a given analyte i can be expressed with the following fundamental thermodynamic equation:

$$\ln k_i = -\frac{\Delta H_i}{RT} + \frac{\Delta S_i}{R} + \ln \Phi \quad (1)$$

where k_i is the retention factor, R the universal gas constant, T the absolute temperature in Kelvin, ΔH_i and ΔS_i the molar enthalpy and molar entropy of adsorption, respectively, and Φ the phase volume ratio. Combining Eq. (1) with the expression for the enantioseparation factor ($\alpha = k_R/k_S$, with R arbitrarily referring to the second-eluted enantiomer) and the Gibbs–Helmholtz relationship (Eq. (2)):

$$-\Delta(\Delta G) = RT \ln \alpha \quad (2)$$

gives Eq. (3):

$$\ln \alpha = -\frac{\Delta\Delta H}{RT} + \frac{\Delta\Delta S}{R} \quad (3)$$

This expression relates the temperature and the experimentally easily accessible α value with the molar differential enthalpy ($\Delta\Delta H$) and entropy ($\Delta\Delta S$) of enantioselective adsorption. Provided that these quantities are temperature-independent, which is usually the case, graphical analysis of ln α vs. $1/T$ gives linear plots (van't Hoff plots), from which $\Delta\Delta H$ and $\Delta\Delta S$ can be extracted from the slope ($-\Delta\Delta H/R$) and the intercept ($\Delta\Delta S/R$), respectively.

From a physico–chemical viewpoint, $\Delta\Delta H$ provides information on the relative ease by which the preferentially adsorbed SA enantiomer is transferred from the mobile phase to the immobilized SO of the corresponding CSP. The entropy term $\Delta\Delta S$ is a measure for the changes in the state of order induced by enantioselective SO–SA binding. Negative $\Delta\Delta H$ values indicate an exothermic transfer of the preferentially adsorbed SA enantiomer form the mobile to the stationary phase and therefore a favorable process. Thus, more negative $\Delta\Delta H$ values are ascribed to a more efficient SO–SA transfer and/or stronger interactions with the stationary phase. Negative $\Delta\Delta S$ values, on the other hand, can be interpreted as an increase in order and/or a loss in degrees of freedom due to adsorption and associa-

tion, respectively. Typically, the formation of highly ordered SO–SA associates is accompanied with a significant loss in degrees of freedom and therefore represents a thermodynamically unfavorable process. As a general trend, lower temperatures increase the effectiveness of intramolecular interactions and therefore improve enantioselectivities. However, the loss of entropy might be overcompensated due to desolvation processes that take place (at least partially) prior to SO–SA association. In this less frequently encountered scenario, positive $\Delta\Delta S$ contributions may result and therefore an enantioselective adsorption will be facilitated with increasing temperature.

However, due caution has to be exercised on mechanistic interpretations of thermodynamic parameters derived from retention and enantioselectivity data obtained under linear chromatographic conditions. Generally, CSPs prepared by immobilization of SO molecules onto solid supports comprise enantioselective (es) as well as non-enantioselective (ns) adsorption sites, both of which do contribute to the observable overall retention of the enantiomers ($k_{app,R}$ and $k_{app,S}$ in Eqs. (4) and (5)):

$$k_{app,R} = k_{ns} + k_{se,R} \quad (4)$$

$$k_{app,S} = k_{ns} + k_{se,S} \quad (5)$$

It is important to realize that retention data (k_{app}) of the enantiomeric SAs obtained under linear chromatographic conditions cluster both types of interactions in an inseparable fashion:

$$\alpha_{app} = \frac{k_{app,R}}{k_{app,S}} = \frac{k_{ns} + k_{se,R}}{k_{ns} + k_{se,S}} \quad (6)$$

$$\alpha_{intr} = \frac{k_{se,R}}{k_{se,S}} \quad (7)$$

As is evident from Eqs. (6) and (7), in cases where non-enantioselective retention increments are prominent ($k_{ns} > 0$) the observed enantioselectivity α_{app} is lower than the intrinsic one ($\alpha_{app} < \alpha_{intr}$). In these situations efforts to reveal thermodynamic parameters via van't Hoff analysis of apparent retention data will inevitably lead to erroneous results. Only in cases where the non-selective retention term can be neglected, i.e., $k_{ns} = 0$ or $k_{ns} << k_{se,R}/k_{se,S}$, the experimentally observed α_{app} represents a good measure for α_{intr}.

Addressing these problems, Fornstedt and coworkers [9,10,26] suggested a method for deconvolution of the stereoselective from non-stereoselective retention increments for various analytes on silica-supported protein-type CSPs. The non-enantioselective and enantioselective contributions of each enantiomer could be isolated by establishing accurate adsorption isotherms over an extended concentration range and subsequent fitting of the experimental data to a bi-Langmuir model. Thus it became possible to distinguish between apparent and the significantly larger ''true'' enantioselectivity factors and to determine the corresponding ''true'' thermodynamic parameters.

In the field of enantiomer separation by gas chromatography, Schurig et al. introduced an alternative approach to access the intrinsic thermodynamic parameters of chiral recognition [27–29]. Similar to liquid chromatography, the use of diluted SO systems in gas chromatography gives rise to non-selective SAs interactions with the matrices used as SO solvents. Measuring under identical experimental conditions the retention data of the SAs on a SO-containing ''reactor column'' and a ''reference column'' devoid of SO provides ''chemical retention increments'' which allow to account for the existence of non-selective interactions.

Sophisticated analyses of the retention behavior are particularly indicated with CSPs displaying surfaces with relatively low SO coverages and/or inaccessible SO units, for example, proteins immobilized onto silica type carrier. For these systems, extreme low SO loadings (<1 μmol protein/g) are reported, and the number of enantioselective binding sites is frequently less than one per protein molecule due to restricted accessibility. In addition, protein-type CSPs possess a large number of potentially non-enantioselective binding sites, represented by non-stereoselective regions of the extended protein surface, chemical entities used for attachment and residual silanols of the silica surface, all of them severely obscuring the intrinsic enantioselectivity.

As mentioned above, with enantioseparation systems for which non-stereoselective interactions can be shown to be small or negligible, apparent retention data accessible under linear chromatographic

conditions may provide a valid basis for a mechanistically meaningful analysis of the underlying thermodynamic phenomena. These requirements are fulfilled for the enantioseparation of *N*-acylated amino acids with cinchona alkaloid carbamate type CSPs in buffered hydro–organic mobile phases. Such CSPs are prepared by covalent attachment of cinchona alkaloid carbamates (see Fig. 1) to mercaptopropyl-modified silica gel and subsequent end-capping of residual thiol groups [30,31], leading to high levels of SO coverage (>280 μmol/g) and efficient suppression of non-selective SA interactions with the carrier surface. The mercaptopropyl-modified silica used as platform for SO-attachment shows little affinity to acidic SAs in buffered hydro–organic mobile phases routinely employed to operate cinchona carbamate type CSPs. In fact, a series of control experiments performed on a reference column packed with this carrier material revealed $k<0.1$ for a broad variety of *N*-acylated amino acids

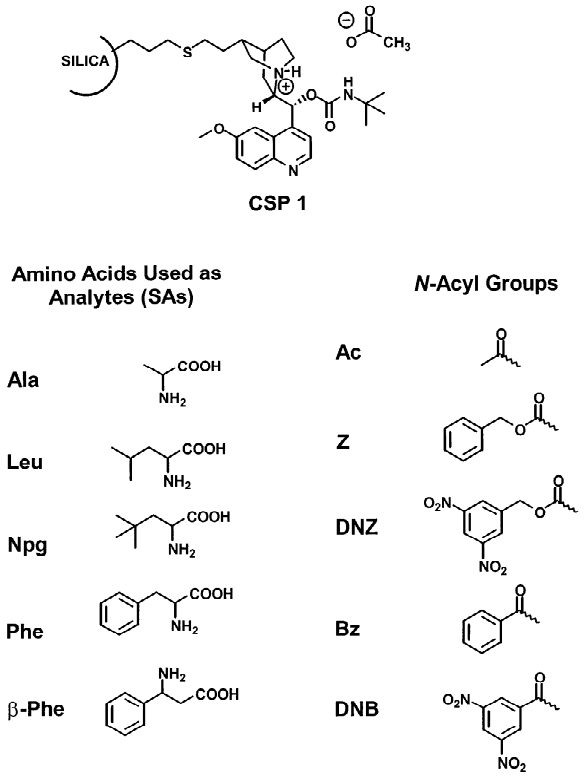

Fig. 1. Chemical structures of CSP 1, the investigated amino acids and the functionalities used for *N*-acylation.

[32]. With cinchona alkaloid type CSPs the retention of acidic SAs is primarily governed by an ion-exchange mechanism [30,31]. Consequently, SAs incapable of undergoing ion-pairing interactions with the immobilized positively charged SO, such as basic and neutral compounds, remain essentially non-retained.

This body of experimental observations provides compelling evidence that selective SO–SA interactions do dominate the retention characteristics of *N*-acylated amino acids on cinchona alkaloid carbamate type CSPs in buffered hydro–organic mobile phases. Thus it can be expected that apparent retention and enantioselectivity data constitute a valid basis to approximate thermodynamically meaningful parameters for the underlying stereoselective adsorption mechanisms.

Along this line, the objectives of the present study are to establish the temperature influence on the apparent retention characteristics and enantioselectivity of a set of *N*-acylated amino acids on a representative quinine carbamate anion-exchange type CSP (see Fig. 1) under linear chromatographic conditions, and to derive the respective apparent thermodynamic parameters by van't Hoff analysis. Based on these experimental data, the influence of specific structural features of these SAs on apparent thermodynamics of enantioselective adsorption will be discussed in the light of mechanistic aspects of chiral recognition.

2. Experimental

2.1. Materials

All chemicals used were of analytical grade. Methanol (HPLC gradient grade) and ammonium acetate were purchased from Merck (Darmstadt, Germany). Glacial acetic acid and racemic alanine (Ala), leucine (Leu), phenylalanine (Phe) and neopentylglycine (Npg) were purchased from Fluka (Buchs, Switzerland). As supporting matrix for CSP 1 spherical silica (Kromasil 100) with a mean particle size of 5 μm and a specific surface area of 314 m^2/g from Akzo Nobel (Bohus, Sweden) was used. β-Phenylalanine (β-Phe) was prepared following a literature procedure [33]. *N*-Acylated amino

acids depicted in Fig. 1 were available from prior studies [31,34] or were prepared following well-established Schotten–Baumann type acylation protocols.

2.2. Chiral stationary phase (CSP 1)

CSP 1 (see Fig. 1) was prepared by immobilization of quinine *tert*.-butylcarbamate to mercaptopropyl modified silica and subsequent end-capping of the residual thiol groups [30]. The selector loading (280 μmol/g) was calculated based on the nitrogen content determined by elemental analysis. CSP 1 was packed into a 150×4 mm I.D. HPLC column using a standard slurry packing protocol (Forschungszentrum Seibersdorf, Austria).

2.3. Chromatography

2.3.1. Instrumentation

The HPLC system consisted of an L-7100 intelligent pump, an L-7400 UV–visible spectrophotometric detector, an L-7200 autosampler and D-7000 interface and the chromatographic data were processed using HSM 7000 chromatography data station software (Merck).

2.3.2. Variable-temperature chromatography

To establish isothermal conditions, CSP 1 was immersed in a thermostatically controlled water–2-propanol bath connected with a thermostat, Model F6-C40 (HAAKE, Karlsruhe, Germany), allowing temperature control with an accuracy of ±0.1 K. After each temperature change, the mobile phase was allowed to pass through the column for at least 1 h prior to analysis to assure equilibrium conditions.

The mobile phases (MPs) contained methanol–aqueous ammonium acetate (80:20; v/v). The final concentration of ammonium acetate was 0.02 *M* (MP 1, used for acetyl-, Z-, Bz-, and DNZ-amino acids) and 0.2 *M* (MP 2, used for *N*-DNB-amino acids), respectively. The apparent pH (pH_a) was adjusted to 6.0 by addition of appropriate amounts of acetic acid. To account for pH-shifts due to temperature changes, the pH values of MP1 and MP2 were adjusted at the corresponding operation temperatures. All these pH measurements were performed with a temperature-resistant SenTix 61 electrode (WTW Weilheim, Germany, pH 0–14), allowing an operation range of 0–100 °C with an accuracy of ±0.01 pH units. Chromatographic runs were performed with the analytes depicted in Fig. 1 at column temperatures of 0, 12.5, 25, 45, 65 and 85 °C. For all runs, the flow-rate was 1 ml/min and signals were detected at 230 nm. The injected sample volume was 20 μl of a solution containing 2 mg/ml analyte in the corresponding MP. Void volumes were determined at each temperature using thiourea as non-retained marker. Linear regression analysis of the van't Hoff plots was performed using Origin 3.01 (MicroCal).

3. Results and discussion

It should be stressed that in the following discussions the terms *enantioselectivity* and *retention* refer to *apparent* experimental data derived under linear chromatographic conditions. A deconvolution of non-selective and selective retention data has not been attempted, but for reasons outlined in the introductory section (see above) it is assumed that non-selective increments are to be neglected under the experimental conditions used. Nevertheless, the *relative* thermodynamic parameters ($\Delta\Delta H$ and $\Delta\Delta S$, respectively) derived thereof should be understood as useful guiding ''estimates'' to extend the structure-based mechanistic picture of chiral recognition rather than accurate measures of the intrinsic values.

3.1. Van't Hoff plots of apparent retention (k) and enantioselectivity factors (α)

The enantioselectivity of *N*-acylated amino acid derivatives on anion-exchange type CSP strongly depends upon the column temperature. A significant improvement of enantioselectivity was observed for most SAs at subambient temperatures. Thus, if the column temperature was reduced from 25 to 0 °C, most α values increased by a factor of about 2 (see Fig. 2).

This strong temperature effect was the motivation for an extensive study dealing with thermodynamics of enantiomer separations of various *N*-acylated amino acids. Enantioselectivity values were determined at six different temperatures in a range between 0 and 85 °C. Increasing temperatures led to

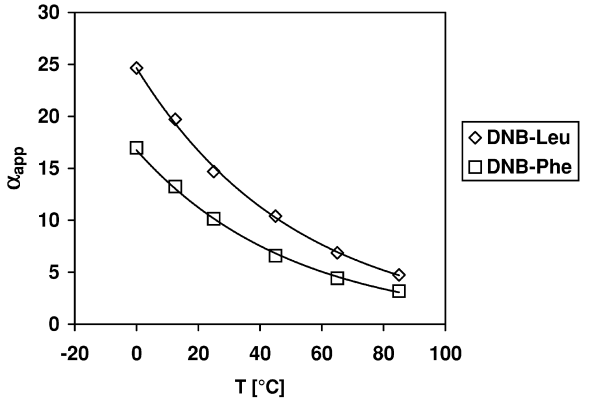

Fig. 2. Temperature dependence of the enantioselectivity factors of DNB-Leu and DNB-Phe on CSP 1. For chromatographic conditions see Table 1.

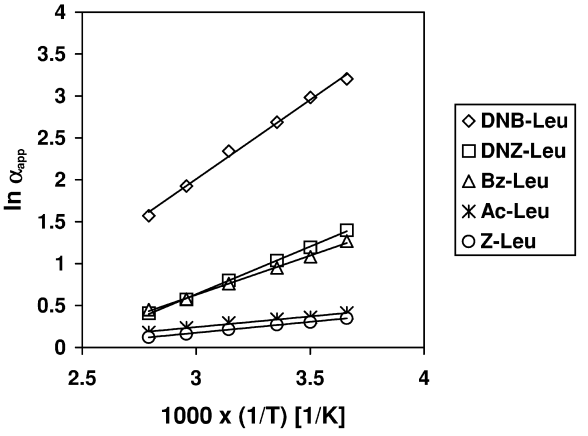

Fig. 4. Van't Hoff plots for the apparent enantioselectivity factors of various *N*-acylated leucine derivatives obtained with CSP 1. For chromatographic conditions see Table 1.

diminished enantioselectivity and reduced retention. As a general trend, van't Hoff analysis of the retention factors (ln k vs. $1/T$) gave pronounced non-linear plots (see Fig. 3). In contrast, ln α vs. $1/T$ plots showed linear behavior over the investigated temperature range as depicted in Fig. 4. From this observation it becomes evident that the factors causing non-linearity for ln k plots affect the retention of both enantiomers to the same extent, suggesting that the origin of this phenomenon is unrelated to chiral recognition processes. Closer inspection of the ln k vs. $1/T$ plots reveals a rather linear van't Hoff behavior between 0 and 25 °C, but, above this range the slopes decrease significantly; thermodynamically this means that ΔH values become more negative and thus adsorption of the analytes becomes more exothermic. To rationalize this unexpected behavior qualitatively, the crucial role of ionic interactions in SO–SA binding has to be considered. Intermolecular association of the anionic SAs with the cationic SO can be broken down in the following sequential subprocesses: (i) desolvation and removal of the electric double layer of SA and SO; (ii) establishment of concerted electrostatic, van der Waals and hydrophobic interactions between the

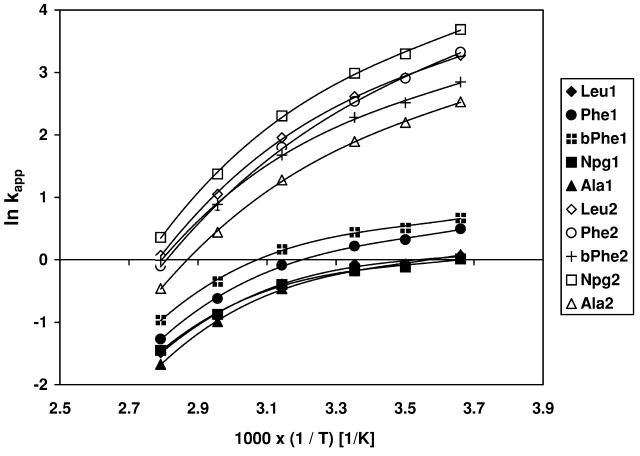

Fig. 3.. Non-linear van't Hoff plots of the apparent retention factors for DNB derivatives obtained with CSP 1. For chromatographic conditions see Table 1.

SO and SA; (iii) possible association-induced conformational rearrangements of SA and/or SO, and finally (iv) re-solvation of the formed diastereomeric adsorbates.

Among these processes, thermally induced removal of counterions or solvent molecules from the SO and/or SAs may account for the observed non-linearity of the ln k plots [21]. Clearly, this effect would decrease the energetic costs that are needed to rearrange the well-structured solvent- and/or counterion-spheres of SA and SO prior to complex formation, hence the overall adsorption enthalpy would become more negative, as observed in the present case. These temperature-dependent desolvation phenomena would be expected to affect both enantiomers in a very similar way and thus being in agreement with the linear van't Hoff behavior of the α corresponding values.

3.2. Correlation between specific structural features of the analytes and the thermodynamic functions of enantioselective adsorption

The non-linear van't Hoff behavior observed for the retention factors certainly precludes a detailed study of thermodynamic parameters associated with the adsorption of the individual SA enantiomers and the immobilized SO. However, the linearity of the corresponding ln α vs. $1/T$ plots suggests that the *relative* energetics of enantioselective adsorption (i.e., $\Delta\Delta G$ values) follow well-defined thermodynamic rules. It should be pointed out that the following discussions are based on *relative* thermodynamic parameters, with the understanding that they might reflect incremental structure-based aspects rather than a comprehensive picture of the underlying retention mechanisms.

In order to create a rational basis for a qualitative analysis of the individual thermodynamic contributions to chiral recognition of *N*-acylated amino acids by the SO unit and CSP 1, respectively, a set of SAs with specific structural features was investigated. These amino acid derivatives are depicted in Fig. 1. To ensure readily interpretable results, amino acid side chains were chosen to display relatively hydrophobic groups with different size, shape, electronic properties and conformational flexibility. Different degrees of steric preorganization and π-donor–acceptor properties were the criteria to select the corresponding *N*-acyl and carbamoyl groups. In the following two chapters, trends related to side chain effects and nature of the *N*-acylation groups will be discussed separately.

3.2.1. Influence of the N-acyl group

The nature of the acyl and carbamoyl groups in the SAs has obviously a strong influence on thermodynamics of enantioselective adsorption to the quinine *tert*.-butylcarbamate type SO. Retention and enantioselectivity data for 298 K and the thermodynamic quantities $\Delta\Delta G$, $\Delta\Delta H$ and $\Delta\Delta S$ for the investigated amino acid derivatives are listed in Table 1. As a general trend, SAs with pronounced π-acidic functionalities, e.g., DNB and DNZ groups, interact more strongly with the SO, while those with Z- and Ac-moieties exhibit much weaker affinities. The enantioselective binding of DNB-amino acids is characterized by highly negative $\Delta\Delta H$ values, ranging from -10.7 to -15.7 kJ/mol. Replacing the DNB group by the electronically very similar, but spatially extended and conformationally more flexible DNZ-functionality, leads to a 30–50% reduction in interaction energy ($\Delta\Delta H$ values: -5.5 to -10.5 kJ/mol). A similar behavior is observed for Bz derivatives, which are structurally quite closely related to DNB congeners but carry a less π-acidic aromatic subunit. These observations suggest that the *N*-acyl groups of the SAs are actively involved in the chiral recognition process. Evidently, the high level of steric preorganization and the pronounced π-acceptor qualities provided by the DNB system are crucial for highly enantioselective binding to the immobilized SO.

As already outlined above, the overall thermodynamics of SO/SA-adsorbate formation may reflect contributions of the following four processes: desolvation, complex formation, conformational changes, and re-solvation of the formed diastereomeric adsorbates. In the initial phase of the binding event, partial desolvation of both the SO and SA in combination with conformational changes of the SO and/or the SA must take place so that the interaction sites can approach each other for complex formation. Desolvation involves the removal not only of solvent molecules, bound to both the (*R*)- and (*S*)-SAs and SO, but also of acetate ions that compete with the

Table 1
Apparent retention factors, enantioselectivity factors, elution order and thermodynamic quantities of the enantiomer separation of *N*-acylated amino acids on the CSP 1[a]

SA	$k_{1\ app}$	$k_{2\ app}$	α_{app}	e.o.[b]	$-\Delta\Delta G^{298}$ (kJ/mol)	$-\Delta\Delta H$ (kJ/mol)	$-\Delta\Delta S$ J/(mol K)	Q[c]
DNB-Npg[d]	0.9	19.8	23.2	*S*	7.73	15.70	26.73	1.97
DNZ-Npg	4.7	14.0	3.0	*S*	2.72	10.52	26.15	1.35
Z-Npg	2.7	3.6	1.33	*S*	0.70	2.43	5.81	1.40
Bz-Npg	2.2	7.0	3.22	*S*	2.89	10.15	24.34	1.40
DNB-Leu[d]	0.9	13.7	14.7	*S*	6.73	14.09	24.78	1.91
DNZ-Leu	4.2	12.3	2.82	*S*	2.57	9.47	23.14	1.37
Z-Leu	2.5	3.3	1.31	*S*	0.66	2.17	5.05	1.44
Bz-Leu	2.3	5.9	2.58	*S*	2.38	7.79	18.14	1.44
Ac-Leu	1.5	2.1	1.40	*S*	0.83	2.11	4.32	1.64
DNB-Ala[d]	0.8	6.7	7.93	*S*	5.08	11.33	20.97	1.81
DNZ-Ala	4.4	8.4	1.88	*S*	1.57	6.44	16.35	1.32
Z-Ala	2.7	3.2	1.19	*S*	0.41	1.20	2.64	1.52
Bz-Ala	2.2	3.8	1.77	*S*	1.38	4.04	8.93	1.52
DNB-Phe[d]	1.2	12.6	10.10	*S*	5.68	15.25	32.08	1.59
DNZ-Phe	6.9	14.1	2.03	*S*	1.69	6.15	14.97	1.38
Z-Phe	4.6	5.7	1.24	*S*	0.51	1.52	3.39	1.51
Bz-Phe	3.8	7.6	1.98	*S*	1.67	5.76	13.69	1.41
Ac-Phe	2.5	3.5	1.42	*S*	0.83	2.33	5.04	1.55
DNB-β-Phe[d]	1.6	9.8	6.26	*R*	4.46	10.71	20.95	1.71
DNZ-β-Phe	4.1	7.8	1.89	*R*	1.55	5.48	13.19	1.39
Z-β-Phe	2.4	2.7	1.14	*R*	0.32	0.77	1.53	1.69
Bz-β-Phe	2.6	4.3	1.66	*R*	1.25	3.24	6.67	1.63
Ac-β-Phe	1.4	1.7	1.26	*R*	0.52	1.06	1.82	1.95

For the structures of the analytes (SAs) and CSP 1 see Fig. 1.

[a] Chromatographic conditions: stationary phase: CSP 1 (150×4 mm I.D.); mobile phase: methanol–water (80:20, v/v), 0.02 *M* ammonium acetate, pH_a 6.0; flow-rate: 1 ml/min; detection: UV at 230 nm; $T=298$ K.

[b] e.o.: Absolute configuration of the second-eluted enantiomer.

[c] $Q=\Delta\Delta H/(\Delta\Delta S\times 298\ K)$.

[d] Mobile phase: methanol–water (80:20, v/v), 0.2 *M* ammonium acetate, pH_a 6.0.

SAs for the specific ionic site of the immobilized and positively charged SO. This energetically costly process (positive $\Delta\Delta H$ values) might be counterbalanced by positive $\Delta\Delta S$ contributions associated with the return of the previously adsorbed solvent/acetate molecules to the bulk mobile phase [20,35]. Potential conformational changes of the SO and (*R*)- and (*S*)-SAs prior to or in course of complex formation may also consume energy in order to rearrange the molecules to an energetically less favorable state. The actual complex formation via multiple intermolecular interactions is generally exothermic, but the corresponding entropic contribution is negative due to the restriction of the SAs on the CSP. The delicate balance between these contributions leads to either enthalpy- or entropy-dominated processes.

As is evident from the data listed in Table 1, enthalpy-dominated separations were observed for all investigated SAs with CSP 1; however, the relative contributions of the enthalpic and entropic terms to the free energy of adsorption depend on the nature of the *N*-acyl groups. As these effects are difficult to visualize directly from the $\Delta\Delta S$ values, the enthalpy–entropy ratios Q $[Q=\Delta\Delta H/(298\times\Delta\Delta S)]$ were calculated and are listed in Table 1. This arbitrary factor represents the relative contributions of enthalpic vs. entropic effects to $\Delta\Delta G$ at 298 K, a

temperature which is most commonly used for chromatographic enantiomer separations. A comparison of the Q values for the individual classes of *N*-acyl derivatives reveals that the enantioselective association of DNB-amino acids with the SO is significantly more enthalpy-driven (Q ranges between 1.97 and 1.59) than for any of the other SAs. This again reflects the ideal electronic and steric preorganization of the DNB system, which facilitates highly stereoselective SO–SA interactions. SAs containing aromatic functionalities other than the DNB group show significantly lower Q values, typically $Q<1.60$. Remarkably, DNZ derivatives show the lowest enthalpy–entropy ratios ($Q=1.32–1.39$). For this class of SAs a major part of the favorable $\Delta\Delta H$ balance is counterbalanced by unfavorable entropic contributions. Clearly, the enantioselective adsorption of DNZ-amino acids has to be associated with unfavorable desolvation processes and/or extensive restrictions of conformational freedom in course of SO–SA binding.

The trend observed for *N*-acetyl derivatives with respect to Q values is less homogeneous. Moreover, due to the lack of aromatic functionalities, the thermodynamics of chiral recognition cannot be discussed isolated from the side chain effects. However, relative to DNZ-, Bz-, and Z-derivatives, enthalpic increments seem to be more important than entropic contributions.

3.3. Influence of the amino acid side chain

Prior investigations of the enantioseparation characteristics of *N*-acyl amino acids on cinchona carbamate anion-exchange type CSPs revealed that both retention and enantioselectivity are strongly influenced by the nature of the side chain of the SAs [30]. These effects are also evident from the thermodynamic parameters of adsorption determined in this study.

For amino acids with alkyl side chains, enthalpy, entropy and free energy of adsorption become more negative as the length and bulkiness of the side chain increase, irrespective of the nature of *N*-acyl group present. An X-ray crystal structure of a most favorable (*S*)-DNB-Leu/tBuCQN complex [30] revealed that in the solid state the DNB-Leu side chain is located in close proximity to the *tert*.-butylcarbamoyl group of the SO. Provided that this complex geometry is maintained under chromatographic conditions, the side chain may also be capable of undergoing complex-stabilizing hydrophobic interactions with the SO in the hydro–organic mobile phase environment. Supportive for this assumption is the fact that the retention of the more strongly bound (*S*)-enantiomers of DNB-amino acids increases in the order Ala<Leu<Npg (see Table 1). Evidently, the enantioselective hydrophobic interaction increment is strengthened as the lipophilic surface of the side-chain is extended. For DNB derivatives, the experimentally derived thermodynamic parameters allow a rough estimation of the gain in ''stereodiscrimination energy'' induced by the addition of a single methylene (or methyl) group to the amino acid side chain at 298 K. For a more convenient visualization of this effect, the $\Delta\Delta H$ and $\Delta\Delta S\times 298$ K (as an energetic measure) values of the DNB derivatives of Ala, Leu and Npg are depicted in Fig. 5. Calculations assuming a simple linear correlation between the gain in $\Delta\Delta H$ and the number of carbon atoms in the side chains of the SAs lead to a favorable enthalpic increment of about -1.0 kJ/mol per carbon. Analogous considerations for $\Delta\Delta S$, however, reveal destabilizing entropic contributions of about -0.5 kJ/mol per carbon at 298 K. Thus, the net gain in $\Delta\Delta G$ due to an extension of the lipophilic domain amounts to -0.5 kJ/mol per carbon.

In the light of the chiral recognition model men-

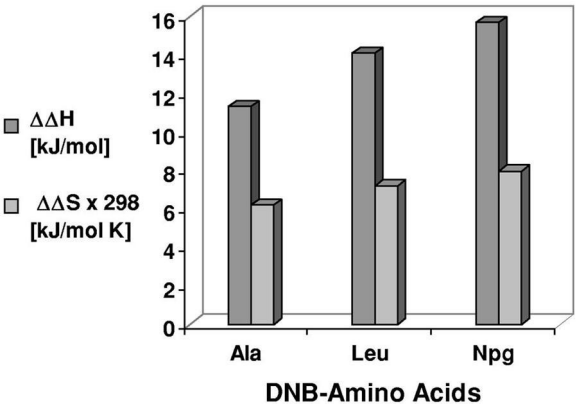

Fig. 5. Effect of increasing side chain size of DNB-amino acids on the relative thermodynamic quantities of enantioselective adsorption ($\Delta\Delta H$, $\Delta\Delta S\times 298$) to CSP 1.

tioned above, the different intermolecular interaction modes of the less strongly bound (*R*)-DNB-amino acids may restrict close side chain-contacts with the *tert*.-butylcarbamoyl group of the SO. In these cases, the complex-stabilizing effects due to hydrophobic SO–SA interactions would be partially or even completely cancelled. Consequently, the overall retention should be diminished and less sensitive to the nature of the side chains present in the analytes. Indeed, small and almost identical retention factors ($k \leq 0.9$) are observed for the (*R*)-enantiomers of the DNB-derivatives of Ala, Leu and Npg (see Fig. 6). The retention data listed in Table 1 indicate similar behaviors for the corresponding DNZ- and Bz-derivatives. Hence, it can be concluded that in hydro–organic media enantioselective hydrophobic binding increments play a prominent role in the chiral recognition process between *N*-acylated amino acids and quinine *tert*.-butylcarbamate type SO.

The thermodynamic parameters suggest a somewhat different behavior for the Phe derivatives. While the enantioselective association of DNB-Phe and the SO is highly favored by enthalpic contributions ($\Delta\Delta H = -15.3$ kJ/mol), this process is associated with the most destabilizing entropic increment ($\Delta\Delta S = -32.1$ J/mol K) in the entire set of SAs. The bi-functional nature of the Phe side-chain, providing hydrophobic as well as π-donor–acceptor interaction qualities, may account for this behavior. The phenyl group might allow for multiple intermolecular interactions and thus for a highly efficient binding to the SO as reflected by the highly negative $\Delta\Delta H$ values. However, the rigidity and the aromatic nature of the side chain might also require extensive conformational rearrangements prior to complexation, leading to an adsorption mechanism with an exceedingly unfavorable entropy balance.

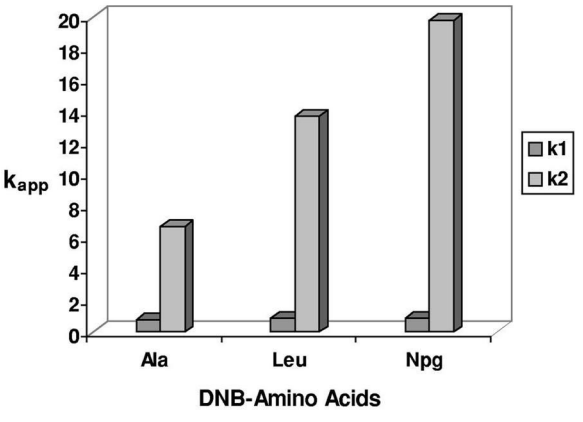

Fig. 6. Comparison of the apparent retention factors ($T = 298$ K) of the first-eluted and second-eluted enantiomers of DNB-derivatives of Ala, Leu and Npg.

A comparison of Phe and β-Phe is useful for the discussion of the different behavior of α- and β-amino acids. Relative to the *N*-acyl derivatives of α-amino acids, the β-congeners are always separated with much lower enantioselectivities on quinine carbamate type SOs [35]. In these SAs, the intramolecular distance between the ion-pairing carboxyl group and the derivatized amino function, capable of hydrogen-bond formation, is extended by a single methylene group only. As can be seen from the corresponding chromatographic data in Table 1, the preferentially adsorbed enantiomer of Phe shows significantly stronger retention than that of β-Phe. A comparison of the respective $\Delta\Delta G$ values reveals that this minor deviation from the ideal ''α-amino acid motif'' diminishes the relative thermodynamic stability of the diastereomeric SO–SA complexes by up to 1.2 kJ/mol. In contrast to α-amino acids, the spatially more extended and conformationally more flexible β-derivatives may allow for fewer and/or less effective intermolecular contacts to be formed between the more strongly retained enantiomer and the relatively rigid binding pocket of the SO. Additionally, the enantioselective binding of β-amino acid derivatives might enforce considerable conformational changes in the SO as well as the SAs, the energetic costs of which would negatively impact on the thermodynamics of binding and adsorption.

3.4. Application-oriented aspects of variable temperature chromatography on cinchona alkaloid carbamate derived CSPs

The results of this study suggest that temperature might serve as a valuable optimization parameter for the enantiomer separation of *N*-acylated amino acids on cinchona alkaloid carbamate anion-exchange type SOs. As stated above, a significant gain in enantioselectivity can be achieved at low column temperatures. Variations of temperature and ion-strength of the mobile phase provide excellent tools for man-

ipulating retention and analysis time. In the case of well-separable DNB derivatives the more strongly retained (*S*)-enantiomer often exhibits exceedingly long retention times, which can be significantly reduced by performing the separation at a higher column temperature. As an example, for DNB-Leu with MP 2 the retention time of the second eluting enantiomer is 54 min at 0 °C, 27 min at 25 °C and 3.5 min at 85 °C.

As a practical consequence, the low temperature conditions might be useful if difficult analytical or preparative separations are projected. For analytical purposes, the enantiomer separations might be performed at 65 °C with mobile phases containing high buffer concentrations, resulting in excellent peak shapes and high resolutions in much shorter time.

4. Conclusions

The variable-temperature enantioseparation characteristics of *N*-acylated amino acids on a quinine *tert*.-butylcarbamate derived CSP, acting as an anion-exchange type SO, has been investigated. With buffered hydro–organic mobile phases at $pH_a = 6.0$ these SAs display pronounced non-linear van't Hoff behavior for the retention factors, but linear van't Hoff plots for the enantioseparation factors.

The enantioselective interaction of *N*-acylated amino acids with the quinine *tert*.-butylcarbamate derived CSP is strongly enthalpy-driven. The thermodynamics of enantioselective adsorption is correlated to structural and electronic properties of the *N*-acyl group and the side chain of the SAs. Generally, the presence of electron-deficient aromatic *N*-acyl substituents and bulky, highly lipophilic side chains enhances enantioselective adsorption, reflecting the importance of intermolecular π-donor–acceptor and hydrophobic interaction with the SO.

As a practical aspect of these studies, temperature has proved to be a powerful tool to control and adjust retention as well as enantioselectivity of acidic SAs on cinchona carbamate anion-exchange type CSPs. For optimization of enantiomer separations, retention and enantioselectivity factors can be varied independently by ionic strength of the mobile phase and column temperature, respectively. While the variation of the ionic strength allows tuning of retention with negligible consequences for enantioselectivity, temperature strongly affects k as well as α values. Subambient temperature chromatography with weak eluents (i.e., low buffer concentration) may be employed to facilitate challenging separations and/or for preparative applications. If short run times are of concern, increased temperatures in combination with mobile phases containing high buffer concentrations are advised.

Acknowledgements

This project was funded by the European Community under the Industrial & Material Technologies Programme (Brite EuRam III, Project # BE 96-3156). The authors are indebted to P. Franco and A. Leitner for the criticl review of the manuscript.

References

[1] U. Beitler, B. Feibush, J. Chromatogr. 123 (1976) 149.
[2] V. Schurig, R. Weber, J. Chromatogr. 217 (1981) 51.
[3] V. Schurig, J. Chromatogr. A 906 (2001) 275.
[4] W.A. König, S. Lutz, G. Wenz, E. von de Bey, J. High Resolut. Chromatogr., Chromatogr. Commun. 11 (1988) 506.
[5] K. Cabrera, D. Lubda, J. Chromatogr. A 666 (1994) 433.
[6] E. Küsters, V. Loux, E. Schmidt, P. Floersheim, J. Chromatogr. A 666 (1994) 421.
[7] K.M. Kirkland, D.A. McCombs, J. Chromatogr. A 666 (1994) 211.
[8] F. Gasparrini, L. Luanazzi, D. Misiti, C. Villani, Acc. Chem. Res. 28 (1995) 163.
[9] T. Fornstedt, G. Götmar, M. Andersson, G. Guiochon, J. Am. Chem. Soc. 121 (1999) 1664.
[10] T. Fornstedt, P. Sajonz, G. Guiochon, J. Am. Chem. Soc. 119 (1997) 1254.
[11] S. Jönsson, A. Schön, R. Isaksson, C. Pettersson, G. Pettersson, Chirality 5 (1992) 505.
[12] A. Karlsson, C. Charron, J. Chromatogr. A 732 (1996) 245.
[13] K. Naemura, J. Fuji, K. Ogashara, K. Hirose, Y. Tobe, Chem. Commun. 24 (1996) 2749.
[14] Y. Machida, H. Nishi, K. Nakamura, H. Nakai, T. Sato, J. Chromatogr. A 805 (1998) 85.
[15] E. Yashima, P. Sahavattanapong, Y. Okamoto, Chirality 8 (1996) 446.
[16] R.J. Smith, D.R. Taylor, S.M. Wilkins, J. Chromatogr. A 679 (1995) 591.

[17] N. Morin, Y.C. Guillaume, E. Peyrin, J.-C. Rouland, J. Chromatogr. A 808 (1998) 51.
[18] T. O'Brian, L. Crocker, R. Thompson, K. Thompson, P.H. Toma, Anal. Chem. 69 (1997) 1999.
[19] E. Papadopoulou-Mourkidou, Anal. Chem. 61 (1989) 1149.
[20] W.H. Pirkle, J. Chromatogr. 558 (1991) 1.
[21] W.H. Pirkle, P.G. Murray, J. High Resolut. Chromatogr. 16 (1993) 285.
[22] J.N. Akanya, D.R. Taylor, Chromatographia 25 (1988) 639.
[23] R.W. Stringham, J.A. Blackwell, Anal. Chem. 69 (1997) 1414.
[24] C. Pettersson, M. Josefsson, Chromatographia 21 (1986) 321.
[25] A. Karlsson, A. Aspegren, Chromatographia 47 (1998) 189.
[26] G. Götmar, T. Fornstedt, G. Guiochon, Chirality 12 (2000) 558.
[27] V. Schurig, M. Juza, J. Chromatogr. A 757 (1997) 119.
[28] V. Schurig, J. Chromatogr. A 906 (2001) 275.
[29] I. Spanik, J. Krupcik, V. Schurig, J. Chromatogr. A 843 (1999) 123.
[30] N.M. Maier, L. Nicoletti, M. Lämmerhofer, W. Lindner, Chirality 11 (1999) 522.
[31] M. Lämmerhofer, W. Lindner, J. Chromatogr. A 741 (1996) 33.
[32] P. Franco, N.M. Maier, M. Lämmerhofer, W. Lindner, unpublished results.
[33] T.B. Johnson, J.E. Livak, J. Am. Chem. Soc. 58 (1936) 301.
[34] V. Piette, M. Lämmerhofer, K. Bischoff, W. Lindner, Chirality 9 (1997) 157.
[35] M. Lämmerhofer, N.M. Maier, W. Lindner, Am. Lab. 30 (1998) 71.